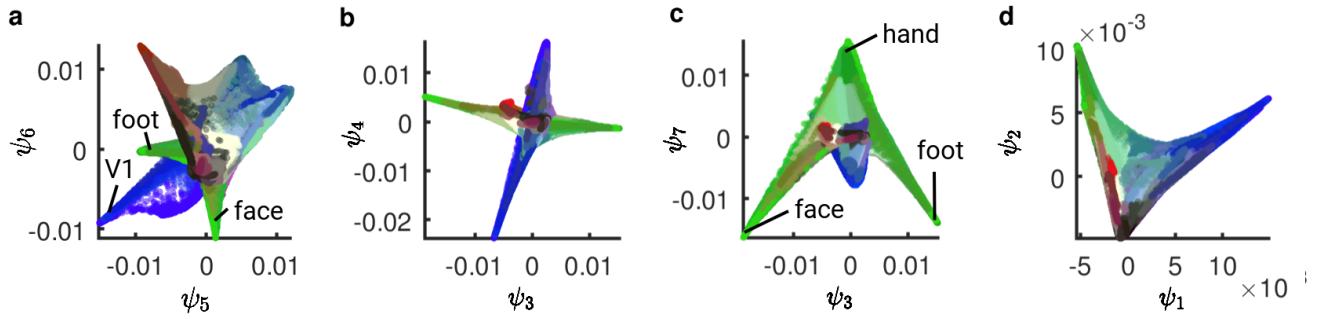


**Cell Reports, Volume 36**

**Supplemental information**

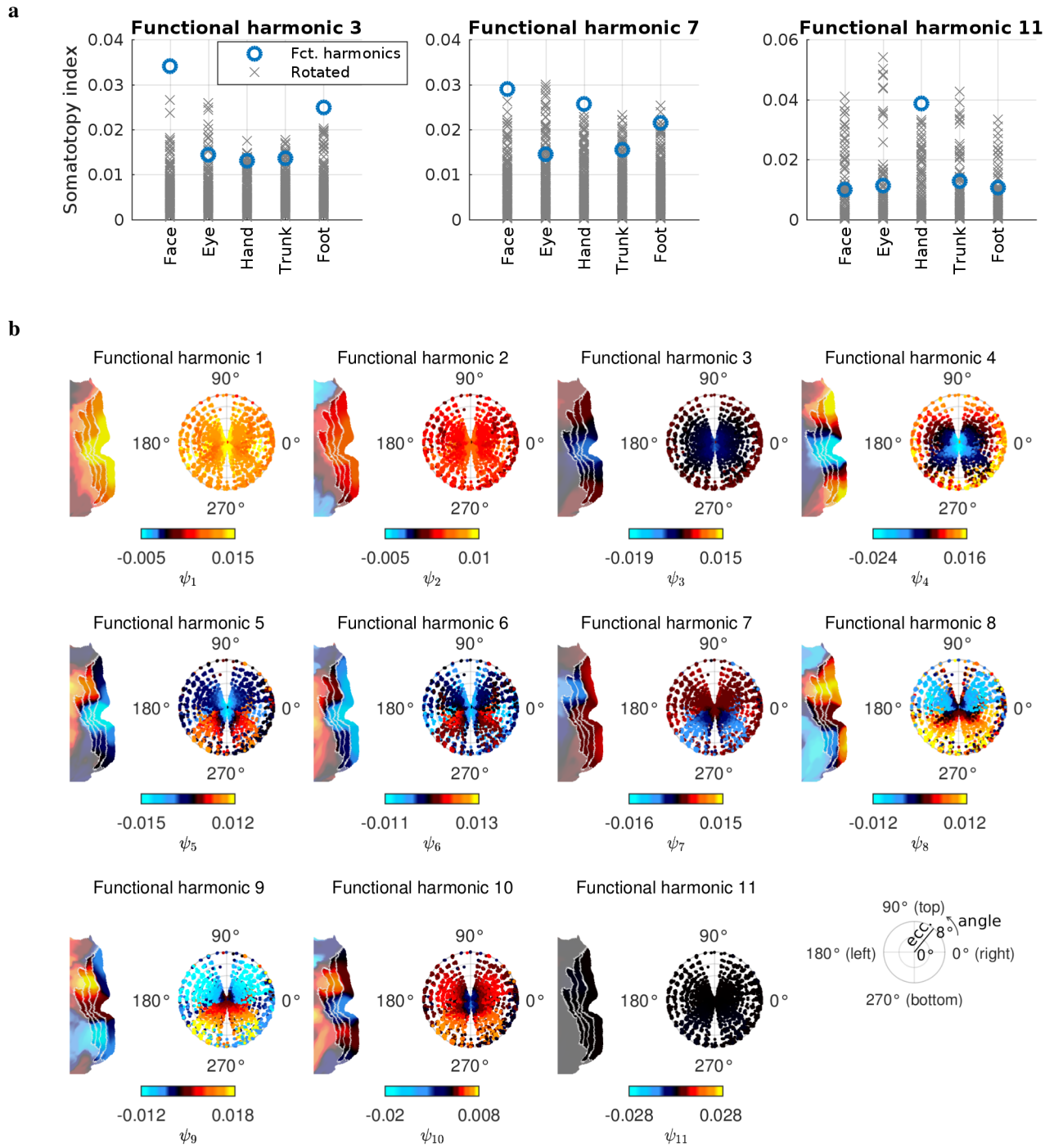
**Functional harmonics reveal multi-dimensional  
basis functions underlying cortical organization**

**Katharina Glomb, Morten L. Kringelbach, Gustavo Deco, Patric Hagmann, Joel Pearson, and Selen Atasoy**

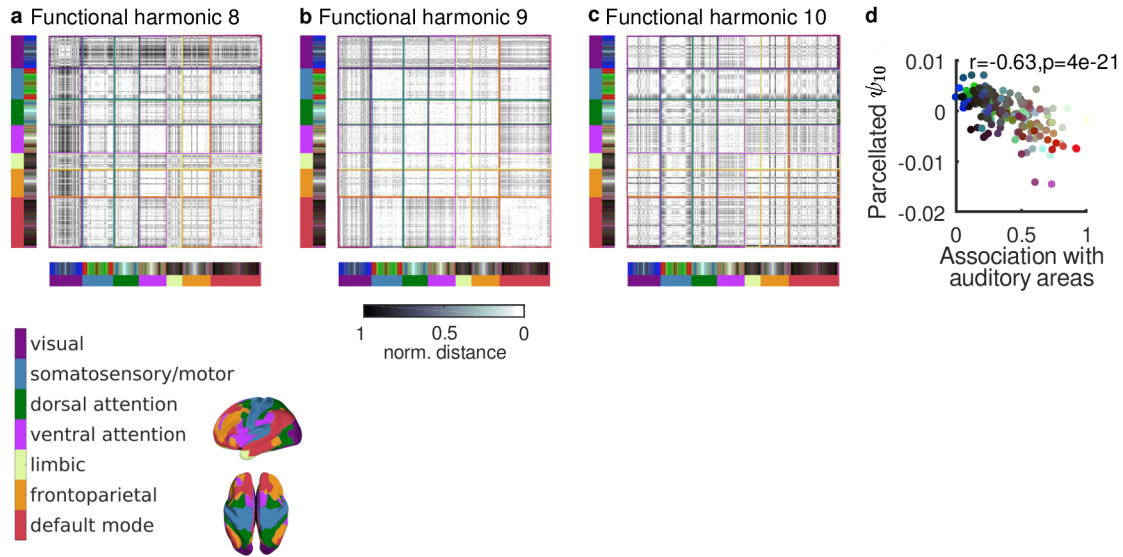


**Supplemental Figure 1. Two-dimensional subspaces formed by pairs of functional harmonics, referred to as  $\psi$ .**

Related to Figure 3. The color code is taken from the HCP parcellation (Glasser et al., 2016), with blue corresponding to visual areas, red, auditory areas, and green, somatosensory/motor areas, and the color gradient running from white to black signifying task-positive to task-negative areas. **a:** Two-dimensional subspace formed by functional harmonics 5 and 6 ( $\psi_5$  and  $\psi_6$ ). V1 (blue), two somatotopic areas (hand and face, green) and auditory areas (red) are separated from each other and from remaining areas. **b:** Two-dimensional subspace formed by functional harmonics 3 and 4 ( $\psi_3$  and  $\psi_4$ ). Visual (blue) and somatosensory/motor/auditory (green and red) systems are orthogonal to each other. **c:** Two-dimensional subspace formed by functional harmonics 3 and 7 ( $\psi_3$  and  $\psi_7$ ). A different separation of somatotopic regions from that shown in Figure 3a is apparent. **d:** Two-dimensional subspace formed by functional harmonics 1 and 2 ( $\psi_1$  and  $\psi_2$ ). This reproduces findings from Margulies et al. (2016), where visual areas (blue), somatosensory/motor areas (green) and higher-order areas belonging to the default mode network (black) are separated from each other. The shown figures are derived from the functional harmonics, obtained from the HCP's dense functional connectivity matrix, which is an average over 812 subjects.

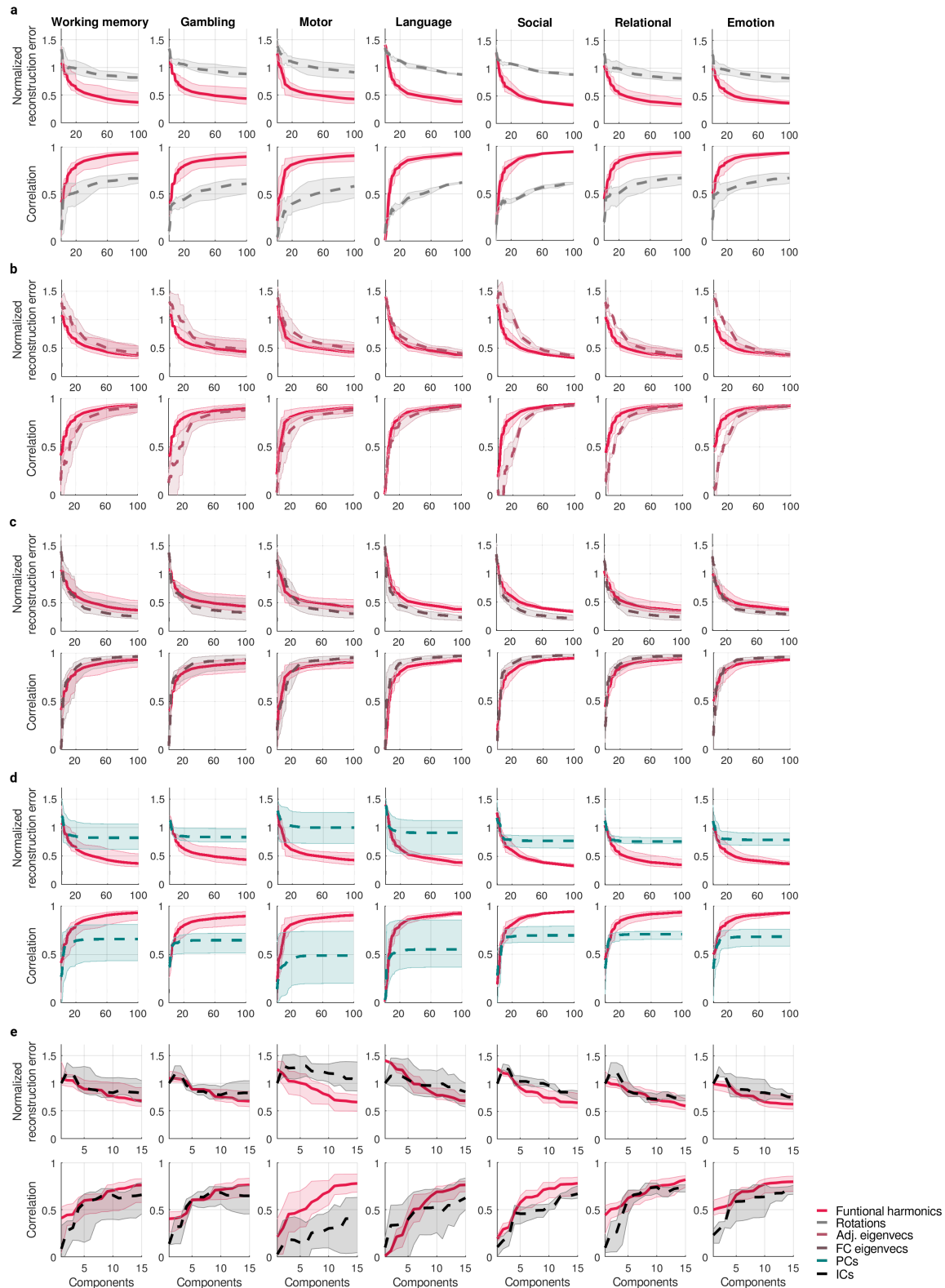


**Supplemental Figure 2. Additional examples for topographical features captured by functional harmonics.** Related to Figure 3b,c. **a:** “Somatotopy index” (see STAR Methods for details) for functional harmonics 3, 7, and 11, and each of the somatotopic subregions (averaged across hemispheres), blue circles; gray crosses are computed from 300 sets of rotations of functional harmonics. This index will be high if the region is separated well from both the entire rest of the cortex and the other somatotopic regions (see Methods). Related to Results-section “Functional harmonics capture sub-areal topographic organization”. **b:** All retinotopic mappings in V1-V4 found in the first 11 harmonics ( $\psi_1$ - $\psi_{11}$ ). The functional harmonics were derived from the HCP’s dense functional connectivity matrix, which is an average over 812 subjects.



**Supplemental Figure 3. Functional harmonics 8-10 correspond to different subdivisions of higher-order networks.**

Related to Figure 2. Normalized average Euclidean distances between all pairs of parcels, ordered by resting state network (RSN) membership according to the Yeo 7-Network parcellation (Yeo et al., 2011; see legend), for functional harmonics 8 ( $\psi_8$ , panel **a**), 9 ( $\psi_9$ , panel **b**), and 10 ( $\psi_{10}$ , panel **c**). **a**: In functional harmonic 8 ( $\psi_8$ ), the distances within the ventral attention network (vATT) are very small, as well as distances between regions belonging to the vATT and the frontal parietal network (FPN). As shown in Figure 4d, we observe a strong retinotopic gradient across regions V1-V4, which is reflected by high distances within the visual RSN. **b**: In functional harmonic 9 ( $\psi_9$ ), most RSNs show small within-network distances, particularly the somatosensory/motor, dorsal and ventral attention, as well as default mode networks. Small distances also occur between the somatosensory/motor and default mode networks. The default mode network (Raichle et al., 2001) is delineated in the positive polarity of this functional harmonic (borders of the DMN as defined by Yeo et al. (2011) are overlaid on functional harmonic 9 ( $\psi_9$ ) in Figure 2i). **c**: In functional harmonic 10 ( $\psi_{10}$ , Figure 3c), only the ventral attention and limbic networks exhibit small within- (but not between-) network distances. **d** Correlation between the degree to which areas are related to auditory regions (Glasser et al., 2016) and the value of functional harmonic 10 ( $\psi_{10}$ ), averaged within each of the 360 parcels. The color code is taken from the parcellation in Glasser et al. (2016), see also Figure 1d. The functional harmonics were derived from the HCP's dense functional connectivity matrix, which is an average over 812 subjects.



**Supplemental Figure 4. Reconstruction performance of functional harmonics (solid lines) compared to control basis function sets.** Related to Figure 5a-g. **a:** Reconstruction performance of functional harmonics compared to their rotations, **b:** eigenvectors of the adjacency matrix, **c:** eigenvectors of the dense FC matrix, **d:** principal components (PCs), **e:** independent components (ICs; dashed lines). Shaded areas show the range (minimum and maximum) of reconstructions errors and (first row of each panel) correlations (second row of each panel) across all tasks in this group. All basis sets were derived from matrices which are averages over the same 812 subjects. The task activity maps (Cohen's D activation contrast maps) are based on 997 subjects.